Phase Averaged Transverse Vorticity Measurements in an Excited, Two-Dimensional Mixing Layer

Peter J. Disimile*
Michigan State University, East Lansing, Michigan

Phase averaged transverse vorticity time series have been obtained in a weakly excited, single-stream mixing layer. The transverse vorticity time series were obtained with an x-array at each of the 414 points in the measurement grid. These data showed the regions of vortex formation, saturation and decay. The spatial locations of the distinctive vortex motions were found to be in good agreement with previous studies: excitation and the relatively thicker boundary layer (approximately 6.5 cm) in the present study was apparently responsible for the larger isolated vortical motions. Using the vorticity field documentation, the spatial distribution and the temporal evolution of the primary vortex motions in the mixing layer were examined. The spatial distribution revealed deep depressions of the vorticity contours on the high-speed side of the mixing layer. The primary growth of the vortical structure was observed to take place on the low-speed side. In addition, observations revealed (over 15% of the available excitation cycle) that the core of the vortical structures appeared to move at substantially different speeds. This detailed documentation of the vorticity field also produced information showing the tearing and fusing of vortical contours in the phase averaged plots.

Background Information

IN a natural (unexcited) free shear layer, vorticity from the boundary layer is continuously shed from a backward facing step. This vortical fluid tends to roll-up (or fold) and to form discrete vortices. The roll-up of the vortical fluid is a result of the natural instability process. For the free shear layer this instability is of the Kelvin-Helmholtz type. For convenience, these naturally occurring discrete vorticies are termed "unit vorticies" in the present discussion.

When periodic excitation is applied (at the separation lip) to a free shear layer, it causes a two-dimensional undulation of the separating boundary layer. This undulation is followed by the agglomeration of the shed vorticity into a large, isolated, vortical structure downstream from the separation lip.[1,2] An efficient agglomeration may be accomplished by exciting the natural shear layer with a low-frequency, periodic disturbance.[3-5]

In addition to agglomeration and nonlinear increases in width, excitation has been found to organize and generate larger vortical structures than would exist in a naturally occurring shear layer. This organization is a result of the vortical structure being "locked" in space with respect to a particular phases (or time) of the excitation mechanism.[3,6]

Using temperature as a passive contaminant, Fiedler and Korschelt[2] measured the transverse space correlation of the temperature fluctuations in a two-dimensional jet. These results reveal a dramatic increase in the space correlation and, hence, in the two-dimensionality of the excited case vs the natural shear layer.

These large vortical motions (or structures) are often referred to as coherent structures. Hussain[7] defines a coherent structure as "a connected, large-scale, turbulent fluid mass with phase-correlated vorticity over its spatial extent. That is, underlying the three-dimensional random vorticity fluctuations characterizing turbulence, there is an organized component of the vorticity which is phase correlated (i.e., coherent) over the extent of the structure." The coherent structure properties can be educed by using phase averaging.

In the foundation work of Mensing,[8] the suppression of pairing of the large, isolated, vortical structure was obtained when the single stream shear layer was weakly excited. Specifically, the mixing layer is said to be weakly excited when a low-frequency disturbance is introduced into the flow with an excitation intensity of

$$\sqrt{\bar{v}'^2}/U_0 \leq 0.0078$$

Under these conditions Mensing found that the subharmonic energy remained approximately one order of magnitude below the energy of the fundamental mode of the structure; this observation reveals that the pairing process, of the large scale motions, is suppressed for these conditions. In addition, Mensing determined that for the case of a weakly excited flow, the vorticies would reach their maximum periodic energy level (become saturated) when the Strouhal number, St_s based on X is approximately equal to 1. The downstream distance where this occurred is referred to as the saturation length.[1,8,9]

The Present Experiment

This study investigated the global vorticity distribution in an excited, plane, mixing layer. The simplest turublent flowfield in which this could be carried out was a nonreacting, single phase, isothermal, two-dimensional, incompressible mixing layer. The single-stream mixing layer, which has a greater spread rate and requires a shorter downstream distance to fully evolve (as compared to that of a two-stream mixing layer) was selected for the present work.

Although weak, periodic excitation organizes the vortical motions in the near field, variations in their downstream location may still exist as a result of phase jitter. Minimization of the effects of phase jitter was accomplished by creating an ensemble of 1000 events (at each spatial location) and subsequently phase averaging these data. To obtain some insight into the possible variations in vorticity as a result of jitter or structure variations (e.g., shape, size, orientation, etc.) the raw data were randomly altered and vorticity redetermined.

Numerous studies have been performed using the technique of flowfield excitation. Therefore, there are many ways to in-

Presented as Paper 85-1648 at the AIAA 18th Fluid Dynamics, Plasma Dynamics and Lasers Conference, Cincinnati, OH, July 14-18, 1985; received July 26, 1985; revision received Jan. 22, 1986.

*Department of Mechanical Engineering. Presently Assistant Professor, Aerospace Engineering and Engineering Mechanics, University of Cincinnati, Cincinnati, OH. Member AIAA.

troduce a periodic perturbation into the flow; among these are the oscillating flap,[10] the vibrating ribbon,[11] and a loudspeaker[6,11] This investigation incorporated the use of a reciprocating piston, to excite the mixing layer. This new method assures a truly two-dimensional, as well as a periodic perturbation.

An excitation intensity of 0.00537 and a Strouhal number St_s (the expected location of the saturated structure) of 0.97 were selected based on Mensing's finding. Setting the excitation frequency f_e equal to 15 Hz, the saturation length x_s was determined to be 84 cm for a freestream velocity (U_0) of 13 m/s. In addition, the approximate number of vorticies that would agglomerate was calculated based on the frequency of the natural instability, f_n. Based on the existence of a turbulent boundary layer (Fig. 1), the following mixing layer relationship was used to relate f_n to the momentum thickness θ; $St_\theta = f_n{}^*\theta/U_0$ where $St_\theta = 0.024$.[12,13] Obtaining f_n enabled the ratio f_n/f_e to be computed, which closely approximated the number of unit vorticies expected to roll-up and form a large, vortical structure. In the present work, approximately three unit vorticies would agglomerate.

Data Acquisition Facility

Direct velocity measurements were made with the use of hot-wire anemometry. Specifically, an x-array was used to measure the velocity at specific locations in the mixing layer. The hot-wires were connected to Disa 55M01 anemometers with a heating ratio of 1.7. In addition, a pitot-static pressure probe monitored the tunnel speed.

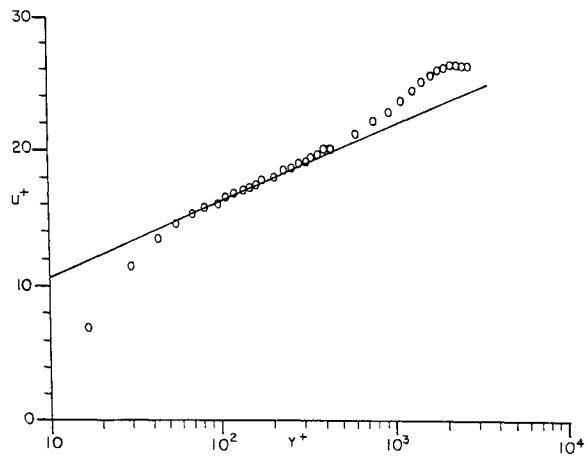

Fig. 1 Law of the wall plot of data at $X = -4.5$ cm, $Z = 0.0$ cm, $\theta = 6.4$ mm, $\delta^* = 8.83$ mm, $u'/U_\tau = 2.63$.

Electronic Signal Conversion/Computer Facility

The analog outputs of the anemometers were input to a TSI 1075X, four channel, simultaneous sample and hold analog-to-digital converter. This 12 bit A/D converter has an input range of approximately 0 to +5V, with a resolution of 1.2 mV (that is, one least significant bit). The external trigger mode was chosen to control the A/D. Therefore, an external device would actuate the A/D on the occurrence of a specific event. This feature of the facility was used in order to provide phase sampled measurements.

The data acquisition system included a computer controlled traversing mechanism. The system, a PDP 11/23 microcomputer and hard disk, enabled a probe to be moved in the X-Y plane and to rotate about the Z-axis.

Experimental Facility and Procedure

Excitation Mechanism

In the present investigation, periodic excitation of the separating, turbulent boundary layer (Fig.1) was required. To accomplish this, an excitation mechanism was designed using a flat, rectangular piston moving in simple harmonic motion.[14] The piston was located immediately downstream of the separation lip and was made to oscillate in the Y direction. The excitation frequency f_e was set at approximately 15 Hz. Fiedler et al.[1] have shown that a precise frequency control is not required since the shear layer response is the same over a wide range of frequencies. Hence, a hand adjusted, electronic motor speed control was used to set the frequency to the nominal 15 Hz. A trip arm attached to the excitation mechanism, working in conjunction with an infrared optical encoder, was used to actuate the A/D converter. The arm was oriented such that the interruption of the infrared beam indicated the relative position of the excitation mechanism. Specifically, the interrupt signal corresponded to the first-phase point (or sample). This occurred when the piston is fully extended in the negative y direction and is equivalent to an angular position of 90 deg on the excitation piston cycle (Fig. 2).

For the present work, under actual test conditions ($U_0 = 13$ m/s and $f_e = 15$ Hz) the excitation intensity $\sqrt{\overline{v'^2}}/U_0$, was determined to be 0.00537.

Data Acquisition Strategy

A measurement grid of 414 node points was established. The rectangular grid was defined by 9 lateral Y locations: $-7.3 \le y \le 17.084$ cm and 46 X (or streamwise) locations: $12.25 \le x \le 149.41$ cm. All mixing layer information was phase sampled with sampling rate of 31.25 kHz. The data were then stored as a phase averaged time series (an ensemble of 1000 events). Each phase averaged time series was 320 samples (or 10.24 ms) long.

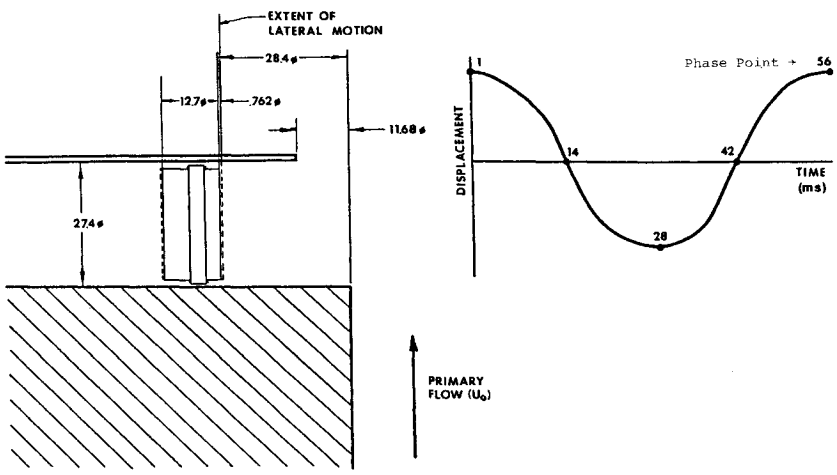

Fig. 2 Schematic representation of excitation mechanism displacement.

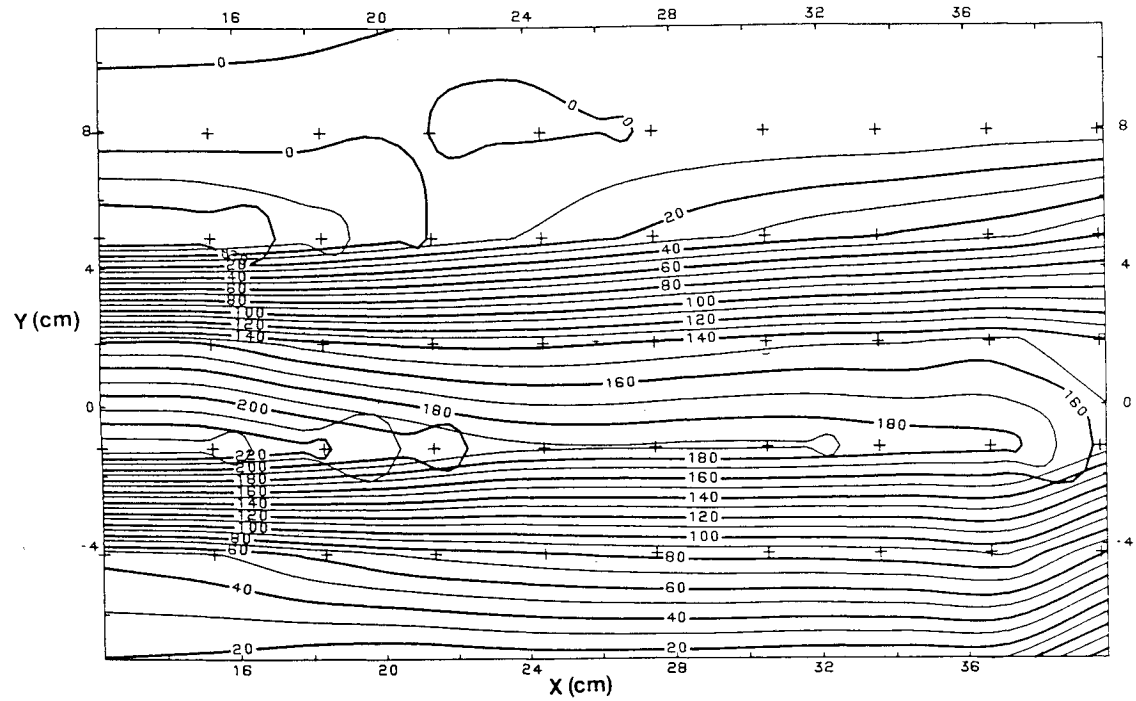

Fig. 3a Phase averaged transverse vorticity $\langle \omega_z \rangle_i$; expanded initial region for $W1$.

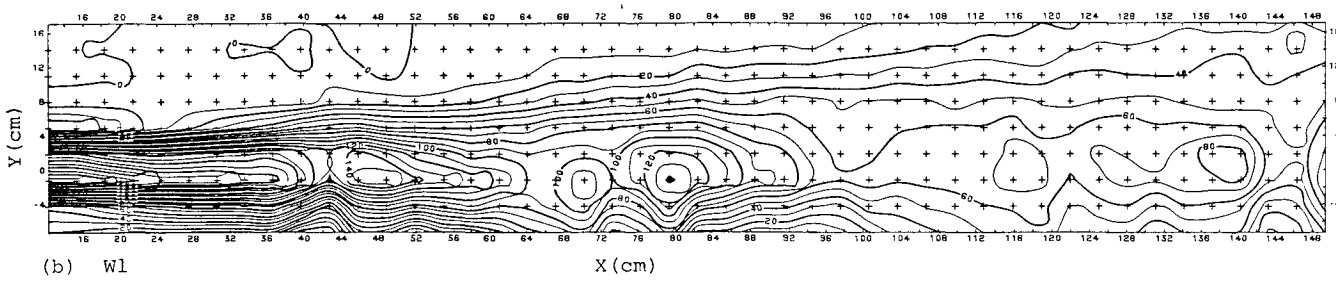

(b) W1

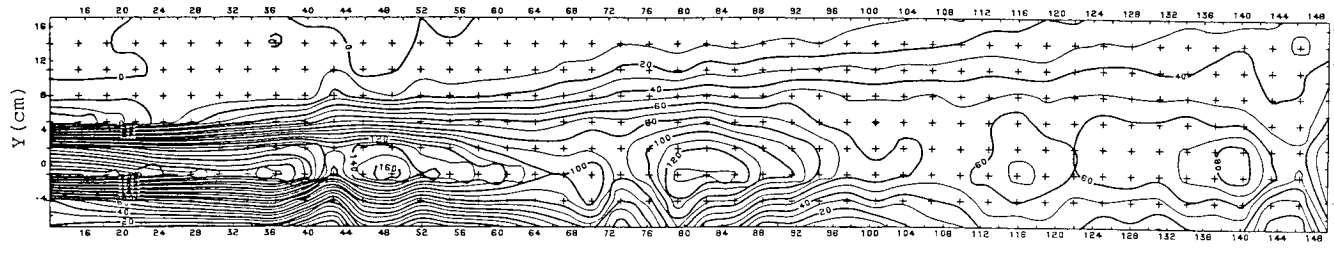

(c) W187

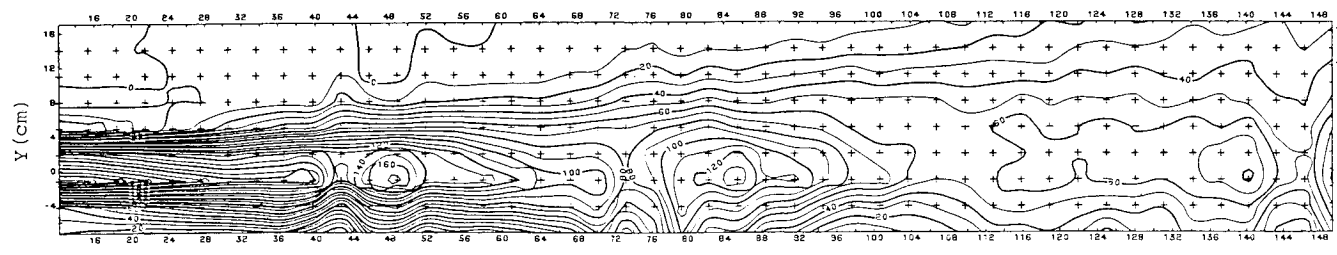

(d) W320

Figs. 3b–d Phase averaged transverse vorticity $\langle \omega_z \rangle_i$.

Results

Spatial Distribution of the Phase Averaged Transverse Vorticity

Once the velocity components ($\langle u \rangle$ and $\langle v \rangle$) were calculated for the complete flowfield, an algorithm fit a cubic equation to the data. The resulting cubic equations were differentiated and the spatial velocity gradients, $\partial\langle u \rangle/\partial y$ and $\partial\langle v \rangle/\partial x$ were evaluated. Using these spatial gradients the phase averaged transverse vorticity was calculated. Figs. 3a-3d represent the phase averaged transverse vorticity contours, depicting the spatial distribution of the vortical motions in the mixing layer at a specific phase point i.

A comparision of the contours obtained at the different phases (times) gave an indication of the temporal changes in the vorticity fields. To allow for easy identification of the vorticity contour lines in the initial region of the excited mixing layer, an expanded view of this region is shown, Fig. 3a. In Figs. 3b-3d, the phase averaged transverse vorticity is plotted for a specific phase of the excitation mechanism. These figures are labeled in such a fashion as to indicate the phase point which they represent. For example, Figs. 3b-3d contain the contours $W1$, $W187$, and $W320$, which represent the phase averaged transverse vorticity obtained at the 1st, 187th, and 320th phase point of the excitation mechanism, respectively.

Phase Averaged Streamwise Velocity Profiles

The phase averaged streamwise velocity component was calculated for each phase point, at all (X-Y) locations and fit with a cubic spline subroutine. The resulting spline equations allowed for the determination of the lateral distribution of non-dimensional velocity. This lateral distribution of the non-dimensional streamwise component of velocity at the last phase point, $\langle U(Y) \rangle_{320}/U_0$ was plotted in Fig. 4 for the following X planes, $X = 24.44$, 39.68, 54.92, 70.16, 85.40, 100.64, 115.88, 131.12 and 146.36 cm.

Perturbed Phase Averaged Transverse Vorticity

The contours of phase averaged vorticity exhibit many interesting features. However, it was recognized that some of the features may be artifacts of the contouring routine or they may result from finite sample size affects. It was considered appropriate to test the sensitivity of the contours to perturbations of the measured voltages.

The strategy used to investigate this sensitivity, was to select random voltage perturbations to be added to the phase averaged voltages ($\langle E_1 \rangle, \langle E_2 \rangle$) at a given ($X$-$Y$) location. The technique used to generate the random perturbations is described below. It should also be noted that the spatial location where the data alteration would occur was randomly selected. This spatial randomness was used to eliminate any bias in the spatial derivatives. The voltages at each of the 414 measurement locations were subjected to the following perturbation process.

The perturbed voltages $\langle E_1^P \rangle$ and $\langle E_2^P \rangle$ were obtained from the phase average voltages $\langle E_1 \rangle$ and $\langle E_2 \rangle$ and the average standard deviations $\bar{\sigma}_1$ and $\bar{\sigma}_2$ by the following (arbitrarily selection) operation:

$$\langle E_1^P \rangle = \langle E_1 \rangle + K^* \bar{\sigma}_1$$

$$\langle E_2^P \rangle = \langle E_2 \rangle + K^* \bar{\sigma}_2$$

where the values of K are a randomly selected multiplier with possible values of 0, ± 0.0625, ± 0.125, ± 0.1875, ± 0.25. The perturbed data files were subsequently input to the vorticity algorithm and the output, perturbed phase averaged transverse vorticity, $\langle \omega_z^P \rangle_i$ was then plotted. Here, only $WP1$ and $WP320$ are shown (Fig. 5).

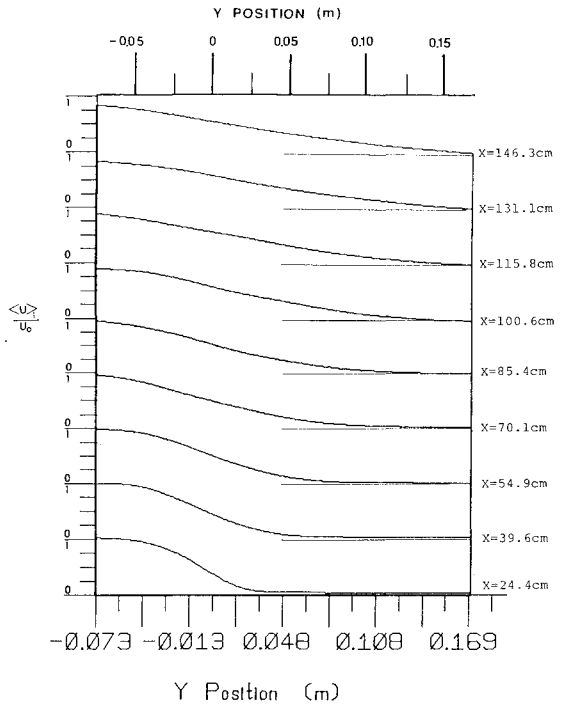

Fig. 4 Phase averaged nondimensional velocity profiles; for phase point, $i = 320$ and at various downstream distances $X = 24.4$, 39.6, 54.9, 70.1, 85.4, 100.6, 115.8, 131.1, 146.3 cm.

Discussion

Vorticity Measurements in an Excited Mixing Layer

This section examines the detailed properties of the phase averaged vorticity field over 15% of the excitation cycle. This vorticity field is created by the excitation of the separating boundary layer of a single stream mixing layer.

The general features of the excited mixing layer have been extensively examined[1,2,6,9]; the present results confirm and extend their observations. A prominent feature of the phase averaged vorticity field is the existence of large scale, vortical motions at some distance downstream from the separation lip. It is important to emphasize that these well-defined vortical structures would not be observed in the time averaged data from an unexcited mixing layer. Such structures, or coherent motions, are known to exist in an unexcited mixing layer, but spatial and temporal irregularity of their occurrence would not allow them to be discerned in a time (or ensemble) average representation of the flowfield. Superimposing the dimensionless phase averaged isotochs and smoke photograph taken at the same phase time, Mensing[8] has shown that the instantaneous and the phase average representations of the flow are in good agreement. This is representative of the repeatability (in the flow behavior) that was created by the excitation process. From Mensing's work the prominent features of the excited mixing layer can be identified: 1) The mixing layer width, as defined by the 0.1 and 0.95 isotoch contours, exhibits a sudden increase at a streamwise distance that is slightly upstream of the first identifiable vortex. 2) As the vortex moves downstream it grows in size and its periodic (or phase average) energy reaches a maximum at a location x_s ($St_s = 1$). At this location the vortical motion is said to be saturated. That is, the vortex has reached the end of the region of amplification and will no longer be amplified. 3) Slightly upstream of the location of saturated structure the mixing layer exhibits another rapid change in width. 4) A thin region of concentrated vorticity exists between the separation lip and the first formed vortical motion. In the present study this region is termed the "tongue."

Only three of the many contour plots of phase averaged transverse vorticity, have been selected for discussion. Each plot represents the phase averaged transverse vorticity field at a phase time i and the plots cover 15% of the excitation cycle. The evolution of the phase averaged transverse vorticity can

be determined by a comparison of the contour plots. In addition, the streamwise component of velocity for several X planes have been included for reference. These considerations are dealt with in the following section.

Phase Averaged Streamwise Velocity

The nondimensional phase averaged streamwise velocity component, is presented in Fig. 4. An examination of these curves indicates the varying slope at the lateral end points of the measurement grid as the profile is plotted at subsequent downstream X planes. The flattening or spreading out of the velocity profiles is apparent downstream of the separation lip.

Spatial Distribution of the Phase Averaged Transverse Vorticity

A phase averaged vorticity contour was obtained for each of the 320 phase points (times), but due to room restrictions only the 1st, 187th, and 320th points are presented (Fig. 3). The following observations were only determined after analyzing data from all 320 phase points. That is, assume 320 photographs were taken of the vorticity field over the entire 414 point measurement grid. Each photo would freeze the flowfield at a specific phase time (point). Therefore, an examination of each plot clearly shows the spatial distribution of several vortical masses. Similarily, as discussed in the next section, a comparison of consecutive contours indicates the temporal evolution of the vorticity field.

Also after a thorough examination of all the vorticity data it has been determined that the crossing of contour lines observed in Fig. 3 and Fig. 5 are a result of the specific plotting routine used. Specifically, this routine is part of the Surface II Graphics software package installed on the Cyber 750 computer at Michigan State University. The insensitivity of these features to random perturbations is discussed in a later section. This insensitivity allows detailed examination of the above aspect with the confidence that the perceived features are not an artifact of the contouring routine. A comparison of Mensing's photograph 3 (see Ref. 8) to the phase averaged transverse vorticity: $\langle \omega_z \rangle_i$, contours obtained in the present work indicate good agreement between the general features of the two flowfields.

A relatively thin region of vortical fluid extending from the separation lip downstream to the newly formed vortical structure is also visible. This relatively thin, highly vortical, region is characterized by 1) the closed vortical contour lines and 2) a slight linear growth of the contour lines upstream of the closure region. As stated previously, this region is termed the tongue.

In the present discussion, Fig. 3c will be used to compare the present work to that of Ref. 1. An examination of this figure indicates that the boundary layer tongue extends downstream to approximately $X=42$ cm or $St_x=0.48$. A rapid change in the width of the lower-level vorticity lines on the low-velocity side of the mixing layer is also observed (see $X=28$ to 33 cm). After this rapid growth, the width of the mixing layer is approximately constant. This region of approximately zero growth continues downstream to the nominal upstream boundary ($X=43$ cm, $St_x=0.496$) of the first fully-formed vortex motion. The location of this first vortex is termed the region of "roll-up" by Fiedler et al.[1] and is preceded by another short segment of rapid growth in the width of the vorticity contours. The center of this first vortex is at $x\approx 48$ cm or $St_x=0.55$. This value is in quite good agreement with the corresponding location ($St_x=0.5$) from the Mensing study.

A region of nominally zero growth exists downstream of the first newly formed vortex. This constant width region is terminated by another region of rapid growth just upstream of the saturated vortical structure. The position of this second vortex ($x_s\approx 85$ cm) is in striking agreement with the equivalent vortex motion (the saturated vortex) that was observed by Fiedler et al.[1] and Fiedler and Mensing.[9] For a weakly excited flow, they found that the nondimensional downstream distance where the saturated structure is located is related to St_x. Interpolating St_x from Mensing's work for a similar excitation intensity the following was obtained:

$$St_s = f_e{}^* X_s / U_0 = 0.97$$

(where $St_s=0.97$ is based on an approximate excitation intensity of 0.0052 as compared to 0.00537 in the present investigation). For the present investigation a $St_s\approx 0.98$ was determined. Farther downstream the periodic energy of the saturated structure starts to decay, with little or no increase in the width of the shear layer. The distance beginning at the location of the saturated structure and extending downstream to a location where the $St_x\approx 1.5$ is termed the decay region by Fiedler et al. For the present work, the decay starts at approximately $X=85$ cm and extends downstream to $X=140$ cm (to the center of the decayed structure). This is equivalent to

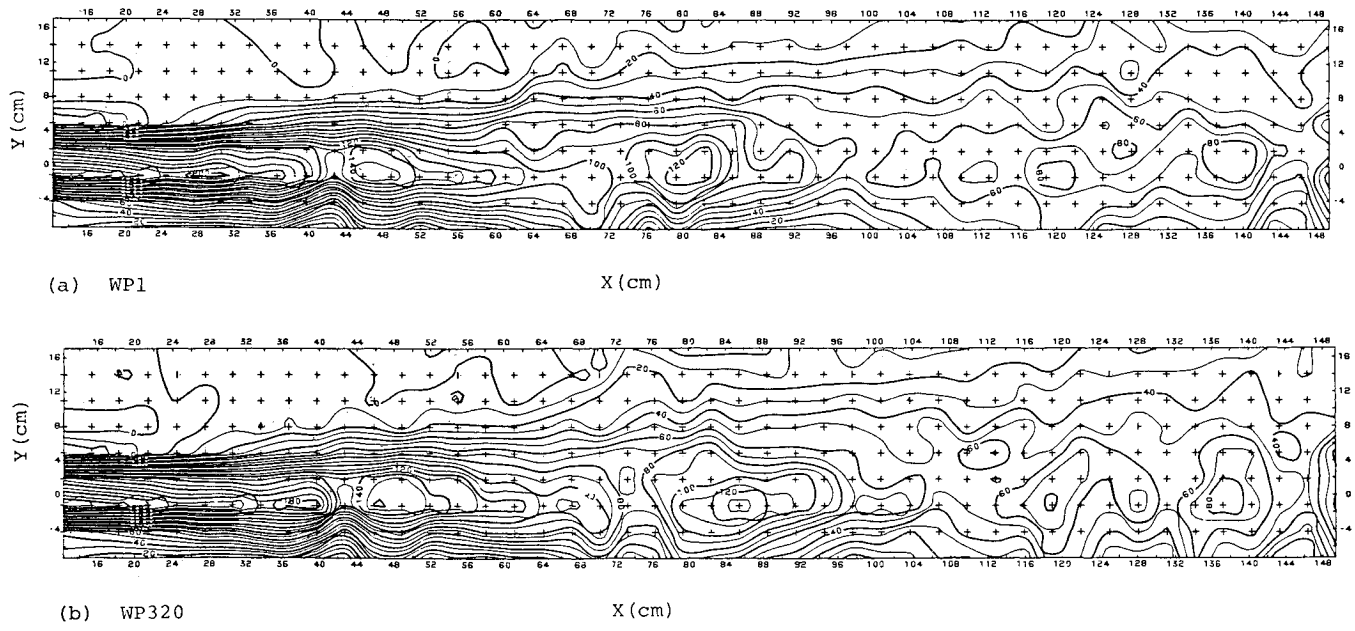

Fig. 5 Perturbed phase averaged transverse vorticity, $\langle \omega_z^P \rangle_i$.

$St_x \approx 1.6$, which differs by 6.6% from the value found by Fiedler et al.,[1] Mensing,[8] and Fiedler and Mensing.[9] At this position, $X = 140$ cm (the end of the decay region), another rapid change in the shear layer width is observed; beyond this position, it is inferred (from the observations by Fiedler et al.[1]) that the shear layer will slowly assume the character of a natural shear layer. Hence, any noticeable effect of excitation is found to persist only up to a streamwise position of approximately 140 cm.

General Temporal Evolution of the Coherent Vorticity Contours

The temporal evolution of the coherent vorticity, $\langle \omega_z \rangle_i$ can be qualitatively obtained by a comparison of Figs. 3b-3d (each contour plot represents a specific phase time i). The detailed observations obtained from such comparisons are listed in Disimile.[14] The following observations are based upon a net evaluation of 320 separate observations.

From the phase averaged transverse vorticity contours it has been observed that in general the lower level vorticity contour lines, on the high-speed side, make deeper depressions into the mixing layer (e.g., $X \cong 42$ cm) than its counterpart on the low-speed side. Accompanying this depression of the vorticity lines is an increase in the phase average lateral velocity $\langle v \rangle$ on the upstream side of the depression by approximately 25% (cf. the $\langle v \rangle$ value of the fluid in the region where the $\langle \omega_z \rangle$ contours are parallel to the X axis). In a complimentary way (after reviewing all of available contours) the growth and shrinkage of the concentrated vortical structure (vorticity values from 80 to 160) appear to be more dominant on the low speed side of the mixing layer.

The average structure velocity was obtained (over the available 15% of the excitation cycles) for the newly formed vortex, the saturated vortex and the decayed vortex. Using the ratio $\Delta L/\Delta t$, the average structure velocity was obtained, where ΔL is the downstream distance a specific vortical structure moved in the time interval Δt:

$$\overline{U_s} = \Delta L/\Delta t$$

Therefore, the average structure velocity ($\bar{U}_s$) was estimated to be 0.70, 5.51, and 1.76 m/s for the newly forming structure, the saturated structure, and the decaying structure, respectively. The average velocity of these vortical motions indicate very little streamwise movement (over the available data which is 15% of the total excitation cycle) by the newly formed vortex ($\Delta x = 0.72$ cm). Yet, the saturated vortex appears to move approximately 5.64 cm in the downstream direction. In a similar manner the concentrated core of the decayed structure moved downstream 1.7 cm. An examination of the streamwise movement of the concentrated core of the saturated structure is presented in Fig. 6. The slope of this curve indicates the core velocity of the saturated structure. These velocities vary an order of magnitude and appear to indicate that the core has undergone periods of large acceleration and deceleration. The positions obtained by this method are estimates, inasmuch as they depend upon the somewhat arbitrary selection of the vortex center. The dashed curve in Fig. 6 is based upon the center of the saturated structure using the perturbed contours. This curve shows greater scatter but the trend is similar to that for the measured data.

In the present work, the writer defines a vortical fluid mass as a local region which is completely enclosed by unbroken contour lines (e.g., the 100 s^{-1} line which completely encloses the core of the saturated structure, $x = 84$ cm). Then the speeds of the upstream and downstream (back and front, respectively) boundaries of these vortical masses can be determined for the available 15% of the excitation cycle. Specifically, the = 3.86 (m/s), respectively. Evidence of this is also found in a flow visualization study performed in an axisymmetric mixing layer by Hussain and Clark.[15]

The lateral location of the boundary layer tongue and of the centers of concentrated vortical fluid appear to be distributed symmetrically around the Y-Z measurement plane where $Y = -1.2$ cm. If a measurement plane were aligned with the separation lip (at $Y = 0$) it is possible that symmetry would exist around that plane. This is a result of the large spatial velocity gradient $[\partial u/\partial y]_{x=y=0}$ that exists at the separation lip and its influence on all points downstream.

There were two dominant vortex interactions observed in the present work: tearing and fusing of vortical fluid masses. A brief summary will be presented herein. The tearing process appears to be related to the deep incursions of the lower level vortical fluid from the high-speed side of the mixing layer. The extent to which the vorticity contour lines are torn and the size of vortical fluid mass which is separated is related to the distance downstream from the separation lip. That is, the farther downstream the structure is located when this tearing process takes place, the more vorticity contour lines are torn and the larger is this separate fluid mass. The fusion process is one in which two or more vortical fluid masses are brought close to each other, fuse and become one fluid mass.

Global Evaluation of the Perturbed and Unperturbed $\langle \omega_z \rangle_i$ Contours

The purpose of this section is to summarize the inferences that are based on the data perturbations described above. The perturbed phase averaged transverse vorticity, $\langle \omega_z^P \rangle_i$ contours were derived in the same manner as $\langle \omega_z \rangle$ with the exception of the random addition or subtraction of a random voltage perturbation to the data before the processing stage.

The spread of the mixing layer in both the perturbed and unperturbed cases are approximately the same. In addition,

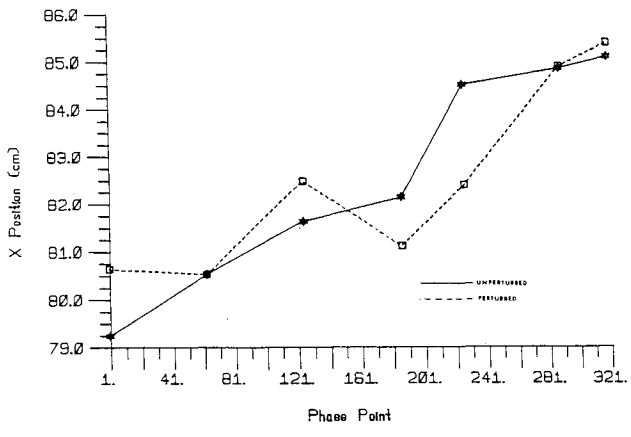

Fig. 6 Streamwise position of saturated structure over 10.24 ms for both the unperturbed and perturbed data.

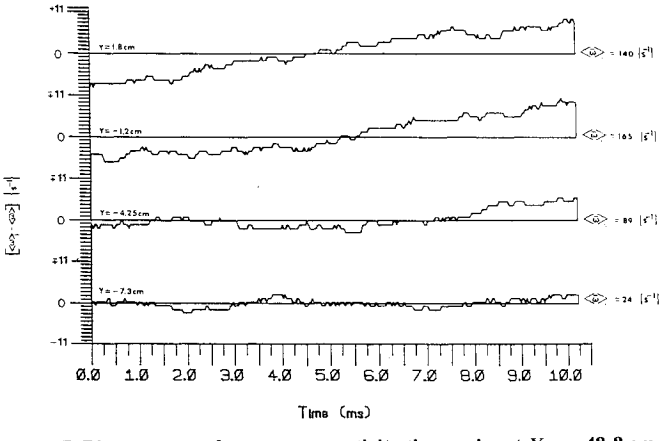

Fig. 7 Phase averaged transverse vorticity time series at $X = -48.8$ cm and $Y - 7.3$, -4.3, -1.2 and 1.8 cm.

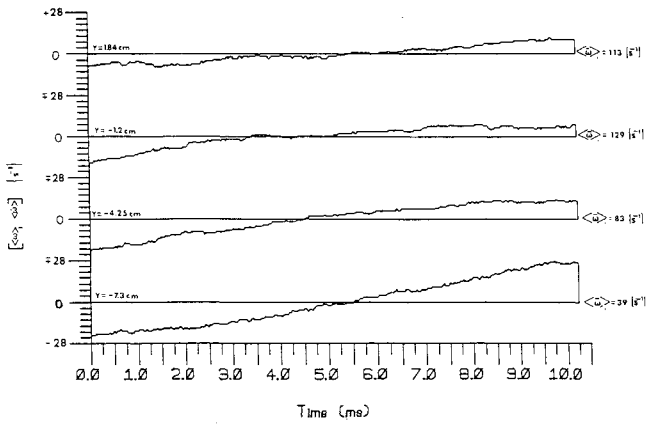

Fig. 8 Phase averaged transverse vorticity time series at $X=85.4$ cm and $Y-7.3$, -4.3, -1.2 and 1.8 cm.

the locations of the concentrated vortical structures are also similar and the vortex interactions observed in the unperturbed case were observed in the perturbed contours. In general, the only differences in the two cases are the magnitudes of vorticity; that is, the level of vorticity in the structures appeared to be greater in the perturbed case, by approximately 10%. The deep depression of lower level vorticity lines in the region between the tongue and the newly formed vortex is also present. Therefore, it can be concluded that in general, on a qualitative basis, the major features, observed in the unperturbed case, are robust results and are not altered by perturbations to the original data.

Phase Averaged Transverse Vorticity Time Series

An investigation into the phase averaged transverse vorticity time series in Figs. 7 and 8, provides quantitative information in support of the events observed in the $\langle\omega_z\rangle_i$ contours.

An examination of Fig. 7 ($x\approx 48$ cm and $Y=-7.3$, -4.25, -1.2, and 1.84 cm) shows the level of phase averaged transverse vorticity variation to be of the same order at the center of this newly formed vortex ($Y=-1.2$ cm) and on the vortex periphery located at $Y=1.84$ cm and considerably reduced at $Y=-4.25$ cm. A similar comparison has been made on the saturated structure (Fig. 8), whose center is located at $x\approx 85.4$ cm (and $Y=-7.3$, -4.25, -1.2, and 1.84 cm). The results indicate approximately the same magnitude of phase averaged transverse vorticity variation at the structure center ($Y=-1.2$ cm) and its peripheries located at $Y=-4.25$ and 1.84 cm. Therefore, it can be concluded from the phase averaged transverse vorticity time series that the center of the saturated structure is relatively calm on the average, and that the $\langle\omega_z\rangle$ variations in the concentrated vortical core is of similar magnitude as the $\langle\omega_z\rangle$ variations on the vortex peripheries.

Conclusions

The prominent features of the phase averaged field (the tongue, the newly formed vortex, and the saturated and decaying vortex) that were observed by Fiedler and co-workers were also observed in the present work. Using the 320th phase point as a representative condition, these last three structures appear at the nominal Strouhal number locations of: $St_x=f_e{}^*X/U_0=0.55$, 0.98 and 1.6, respectively. These values are in good agreement with the corresponding values reported by Refs. 1, 8, and 9.

The phase averaged vorticity contours indicate the deep depression of vorticity lines on the high speed side of the mixing layer. In addition, the dominant growth and shrinkage of the vortical fluid masses seem to be more predominant on the low-speed side of the mixing layer. It has also been observed over the available 15% of the excitation cycle that the cores of the vortical structures move at different speeds. Specifically, the saturated structure appears to move with a much larger average velocity, including periods of relatively large acceleration and deceleration. The existence of vortex interactions, such as tearing and fusing of vortical contours has also been observed.

Acknowledgment

The author would like to express his personal gratitude to his advisor Professor J.F. Foss, and to Dr. M. Rubesin of the NASA Ames Research Center. This work has been supported under a NASA Grant NAG 2-86.

References

[1]Fiedler, H., Dziomba, B., Mensing, P., and Rosgen, T., "Initiation, Evolution and Global Consequences of Coherent Structures in Turbulent Shear Flows," *Lecture Notes in Physics,* Vol. 136, Springer, Berlin, 1980, pp. 219-251.

[2]Fiedler, H. and Korschelt, D., "The Two Dimensional Jet with Periodic Initial Conditions," *Proceedings of the 2nd Symposium on Turbulent Shear Flows,* London, 1979, pp. 18-23.

[3]Wygnanski, I., Oster, D. and Fiedler, H., "A Forced Plane, Turbulent Mixing-Layer; a Challenge for the Predictor," *Proceedings of the 2nd Symposium on Turbulent Shear Flows,* London, 1979, pp. 12-17.

[4]Ho, C.M. and Huang, L.S., "Subharmonics and Vortex Merging in Mixing Layers," *Journal of Fluid Mechanics,* Vol. 119, 1982, pp. 443-473.

[5]Ho, C.M. and Huere, P., "Perturbed Free Shear Layers." *Annual Review of Fluid Mechanics,* Vol. 16, 1984, pp. 364-424.

[6]Fiedler, H., Korschelt, D. and Mensing, P., "On Transport Mechanism and Structure of Scalar Field in a Heated Plane Shear Layer," *Lecture Notes in Physics,* Vol. 76, Springer-Verlag, Berlin, 1978, pp. 58-72.

[7]Hussain, A.K.M.F. "Coherent Structures—Reality and Myth," *Physics of Fluids,* Vol. 26(ID), 1983, pp. 2816-2850.

[8]Mensing, P., 'Einfluss kontrollierter Störungen auf eine ebene turbulente Scherschicht," Dipl.-Eng., Dissertation Hermann-Fottinger-Institut, TU Berlin, 1981.

[9]Fiedler, H. and Mensing, P., "The Plane Turbulent Shear Layer with Periodic Excitation," *Journal of Fluid Mechanics,* Vol. 150, 1985, pp. 281-309.

[10]Oster, D. and Wygnanski, I., "The Forced Mixing Layer Between Parallel Streams," *Journal of Fluid Mechanics,* Vol. 123, 1982, pp. 91-130.

[11]Zaman, K.B.M.Q. and Hussain, A.K.M.F., "Turbulence Suppression in Free Shear Flows by Controlled Excitation," *Journal of Fluid Mechanics,* Vol. 103, pp. 133-159.

[12]Drubka, R.E., "Instabilities in Near Field of Turbulent Jets and Their Dependence on Initial Conditions and Reynolds Number," Ph.D. Dissertation, Illinois Institute of Technology, 1984.

[13]Hussain, A.K.M.F. and Zaman, K.B.M., "Vortex Pairing in a Circular Jet under Controlled Excitation," *Journal of Fluid Mechanics,* Vol. 101, Pt. 3, 1980, pp. 493-544.

[14]Disimile, P.J., "Transverse Vorticity Measurements in an Excited, Two-Dimensional Mixing Layer," Ph.D. Dissertation, Michigan State University, 1984.

[15]Hussain, A.K.M.F. and Clark, A.R., Dissertation, "On the Coherent Structure of the Axisymmetric Mixing Layer; a Flow-Visualization Study," *Journal of Fluid Mechanics,* Vol. 104, 1981, pp. 23-294.